frontiers | Frontiers in Materials

TYPE Original Research
PUBLISHED 04 January 2024
DOI 10.3389/fmats.2023.1323274

OPEN ACCESS

EDITED BY
Zhongya Zhang,
Chongqing Jiaotong University, China

REVIEWED BY
Tao Yan,
Southwest Jiaotong University, China
Luo Gang,
Chang'an University, China

*CORRESPONDENCE
Xiaohan Zhou,
cqzhouxhan@126.com
Ninghui Liang,
lnh83249@cqu.edu.cn

RECEIVED 17 October 2023
ACCEPTED 11 December 2023
PUBLISHED 04 January 2024

CITATION
Liu X, Zhuang Y, Zhou X, Liang N, Mao J and Chen H (2024), Study of the damage characteristics and corrosion mechanism of tunnel lining in a sulfate environment.
Front. Mater. 10:1323274.
doi: 10.3389/fmats.2023.1323274

Study of the damage characteristics and corrosion mechanism of tunnel lining in a sulfate environment

Xinrong Liu, Yang Zhuang, Xiaohan Zhou*, Ninghui Liang*, Jinwang Mao and Hai Chen

School of Civil Engineering, Chongqing University, Chongqing, China

Sulfate corrosion is one of the main causes of tunnel lining deterioration. An accurate understanding of the damage characteristics and corrosion mechanism of sulfate-corroded tunnels is the basis for the anti-corrosion design and damage control of the tunnel lining. Based on a project concerning a sulfate-corroded tunnel in the mountainous area of Southwest China, this study conducted a field investigation and laboratory tests and, combined with existing research data, summarized the damage characteristics and corrosion mechanism of this type of tunnel and proposed the characteristic corrosion state of tunnel lining in a sulfate environment. The results show that 1) sulfate corrosion led to leakage, surface spalling crystallization, and strength loss, and the corrosion typically occurred at the arch waist and arch foot. 2) Physical and chemical corrosion occurred in the tunnel lining, and the corrosion products included sodium sulfate, calcium carbonate, gypsum, ettringite, and thaumasite. 3) In China, this type of tunnel is mainly located in the Southwest and Northwest, and its lining is in a special state of "one-sided accelerated corrosion."

KEYWORDS

sulfate corrosion, lining corrosion, water leakage, strength degradation, one-sided accelerated corrosion

1 Introduction

Concrete corrosion will result in the loss of the bearing capacity of a structure. The lining of a tunnel is an important part of the underground structure. Most of the lining is made from reinforced concrete; therefore, it also faces the problem of concrete corrosion. Up until now, tunnel construction in many countries has passed the period of rapid development and begun to transition to a period of maintenance (Zhang et al., 2019). Thus, lining corrosion problems are a growing concern for scholars all over the world. Among various corrosion factors, sulfate is one of the most important causes of tunnel lining corrosion (Zhuang et al., 2022; Zhang et al., 2023).

At present, there are many reports of tunnels corroded by sulfate. For example, Long et al. (2011) investigated the Fala Tunnel and found that a large number of white crystals were distributed on the lining surface, accompanied by surface spalling and even paste substances. Qi et al. (2005) introduced the phenomenon of salt crystallization and cracking on the lining surface of the Jinjiguan Tunnel. Liu et al. (2023) conducted a damage survey on a highway tunnel in Chongqing that was severely corroded by sulfate and found that the strength of the corroded lining was lower than the designed value. However, the relevant reports were

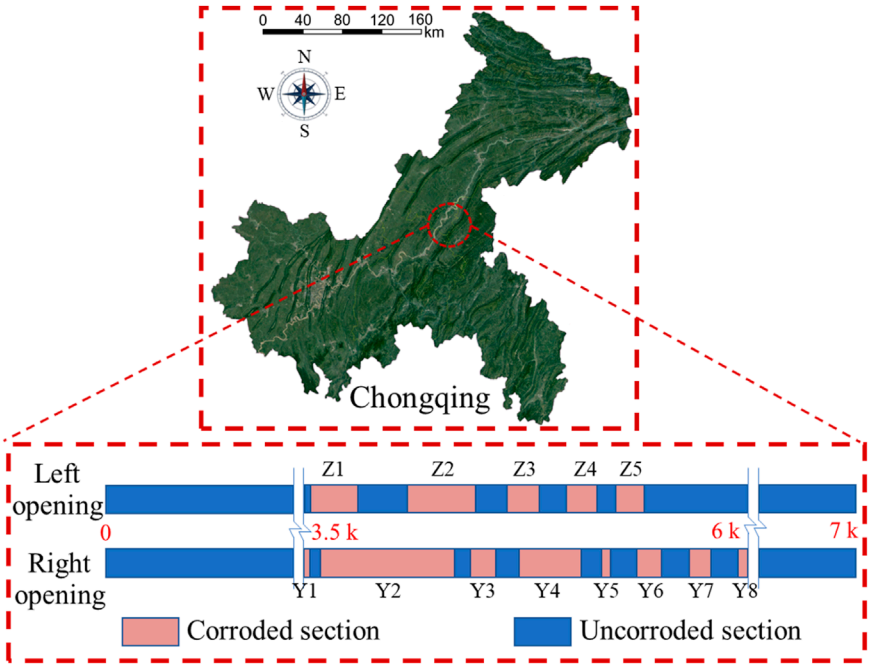

FIGURE 1
Schematic diagram of the location of the damaged tunnel.

mainly focused on a simple description of the service environment of a tunnel and its damage phenomenon, but there is a lack of systematic and comprehensive analysis and summary of the corrosion environment and typical damage characteristics of this type of sulfate-corroded tunnel.

The full-immersion corrosion test is widely used to study the mechanism of sulfate attack on tunnel lining. Results have shown that sulfate chemically reacts with the cement hydration products of concrete, such as calcium hydroxide, calcium silicate hydrate, and calcium aluminate hydrate, and generates insoluble and expansive corrosion products, such as ettringite and gypsum (Hobbs and Taylor, 2000; Crammond, 2002; Lee et al., 2008). These corrosion products will continuously accumulate in the pores of the concrete and generate crystallization pressure on the pore wall. When the expansion stress is greater than the tensile strength of the concrete, serious material cracking and mortar spalling will occur, resulting in a reduction in the concrete bearing capacity (Chen et al., 2008; Ma et al., 2012). However, the actual corrosion condition of the tunnel lining cannot be reproduced in a laboratory environment, and full immersion is not the real corrosion condition of the tunnel lining; therefore, the experimental results cannot capture the real phenomena of tunnel lining corrosion.

Therefore, based on the field investigation and testing of a tunnel severely corroded by sulfate in the mountainous area of Southwest China, this study summarizes the typical damage characteristics of this type of tunnel. Furthermore, a combination with existing tunnel reports corroded by sulfate and the typical working environment of "one-sided accelerated corrosion" of tunnel lining in a sulfate environment was revealed. Finally, the corrosion mechanism was discussed. This study could provide a reference for the corrosion protection design of tunnel lining in a sulfate environment.

2 Damage characteristics of tunnel lining

2.1 Tunnel profile

The project tunnel is an extended tunnel in the mountainous area of Southwest China, with the length of both the left and right openings exceeding 7 km. The distance between the left and right openings of the entrance is approximately 18–10 m, and the distance between the left and right openings of the central section is 30 m. The maximum depth of the tunnel is approximately 650 m. The corrosive ions in the tunnel groundwater are mainly sulfate ions, and the highest concentration reaches 2,775.56 mg/L. The average annual temperature at the location of the tunnel is 16°C–18°C, and the average temperature in the coldest month is 4°C–8°C.

A previous investigation showed that there were a lot of circumferential oblique longitudinal cracks and some network cracks in the secondary lining of the tunnel, and some areas with dense cracks were also the corrosion areas of the lining. Additionally, the rest of the sections were found to be corroded to different degrees in the follow-up investigation. Five years after the grouting treatment of the cracks of a larger width, it was observed that the number of cracks increased again, and the area of corrosion in the secondary lining increased. The corroded sections of the tunnel lining were mainly concentrated in the middle and back sections of the tunnel.

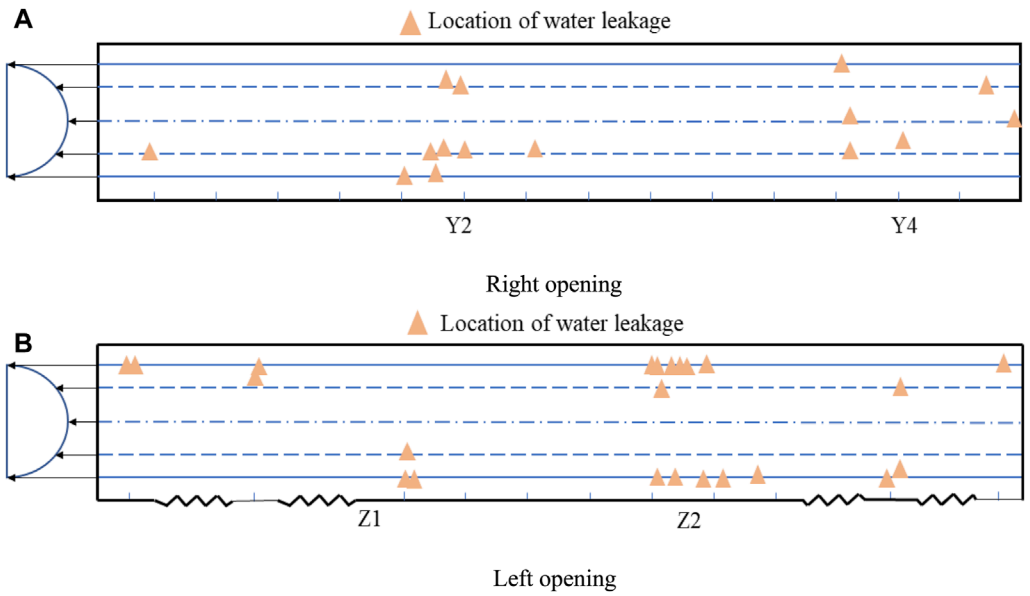

FIGURE 2
Leakage locations in the right opening **(A)** and left opening **(B)**.

As shown in Figure 1, there were five main corrosion sections on the left opening and eight on the right opening.

2.2 Leakage analysis

Water leakage is a common problem in mountain tunnels, with corrosive ions corroding the lining structure. Therefore, first of all, the leakage situation of the left and right openings of the tunnel was comprehensively investigated, the position of the lining leakage section was determined, and the leakage status was observed and recorded. At the same time, a typical leakage section was selected for water quality sampling to detect the concentration of corrosive ions in the water.

As shown in Figure 2, there were 15 leakage points on the right opening and 23 leakage points on the left opening of the tunnel. The leakage mainly occurred at the arch foot of the tunnel, as shown in Figure 3A, then at the arch waist, and occasionally occurred at the vault. Additionally, the leakage was not isolated but usually occurred with cracks and corrosion in the lining, as shown in Figure 3B. Furthermore, no freezing phenomena were observed during the coldest months.

A certain amount of water leakage was collected and analyzed in the left and right openings where the leakage was serious and could be easily sampled. The results showed that the leakage water mainly contained sulfate ions; the concentration of sulfate ions in most of the leakage water was greater than 200 mg/L and the highest was 1,410 mg/L. According to the Code for Durability Design of Concrete Structures in Highway Engineering (JTG T3310-2019), the environmental levels of water in the chemical corrosion environment were divided, and the results are shown in Figure 4. Most of the leakage points in this tunnel were moderately corroded, but in certain places, the degree of corrosion even reached a serious level.

2.3 Lining corrosion

Based on the investigation of the corrosion section of the tunnel, it was found that the corrosion areas were mainly concentrated at the arch foot and waist of the Z1 and Z2 sections of the left opening. This may be because the drainage system of these sections of the tunnel was blocked and corrosive groundwater accumulated in the site, converting the site to a long-term contact site, resulting in lining corrosion.

The corrosion phenomenon is shown in Figure 5. The lining surface, which had a certain strength, was dry and peeled off in large areas, as shown in Figure 5A. Soft white crystals that could be easily removed were present on some parts of the corroded lining surfaces, as shown in Figure 5B. Additionally, the corrosion was deeper in the area of the cracks as shown in Figure 5C. Travertine that was hard and difficult to remove was present in some parts of the cracks, as shown in Figure 5D. Some areas of the arch foot lining were immersed in leakage water, appearing muddy and completely losing their strength, and could be easily observed, as shown in Figure 5E. Cracks and lining corrosion reappeared in some grouting repair sites, as shown in Figure 5F.

3 Testing and results

Owing to the construction period and other factors, we only tested the lining corrosion of the left opening in detail. The strength of the corroded lining was measured using the rebound

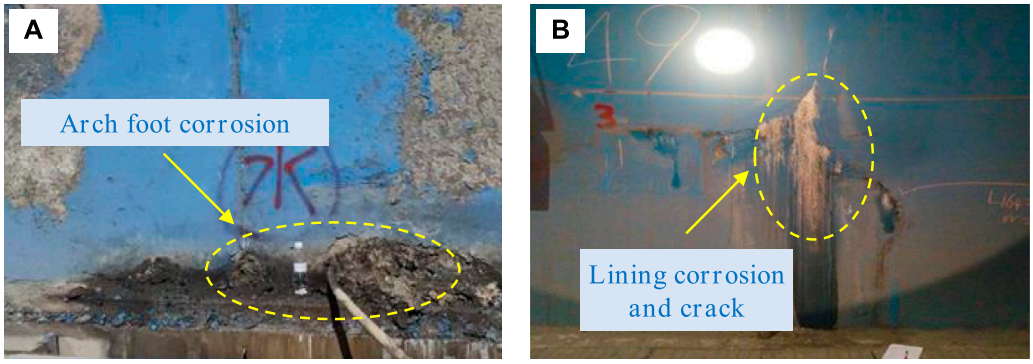

FIGURE 3
Typical tunnel leakage phenomena at the arch foot **(A)** and lining cracks **(B)**.

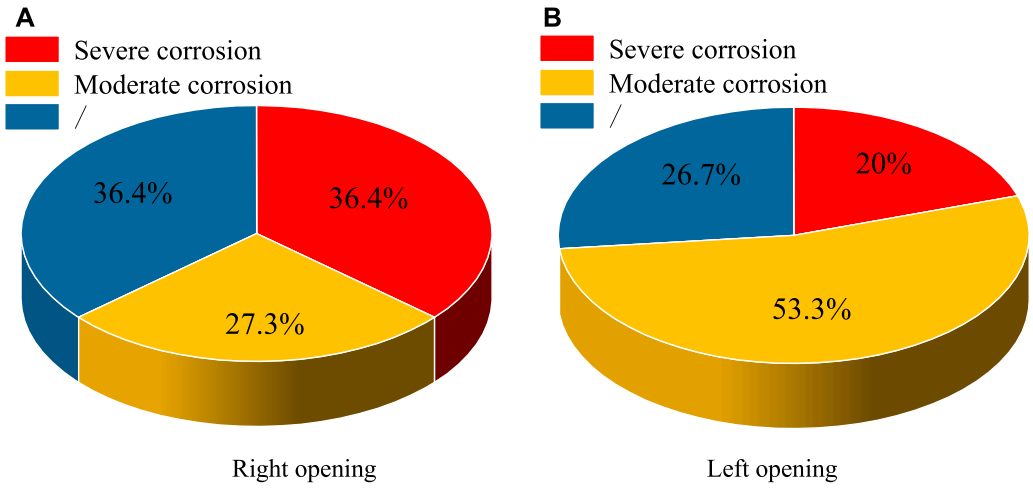

FIGURE 4
Corrosion degree of water leakage in the right opening **(A)** and left opening **(B)**.

method on the areas with a smooth surface and easy to test, and drill holes were used for strength testing in the areas where corrosion was too severe for testing with the rebound method. At the same time, the corrosion products of the tunnel lining were analyzed microscopically to obtain the corrosion mechanism of the tunnel lining.

3.1 Rebound strength test

To facilitate the operation process, 40 test samples in the Z1 section and 63 test samples in the Z2 section were tested to determine the rebound strength. The test methods referred to the Technical Specifications for Testing Concrete Compressive Strength by Rebound Method (JGJ/T23-2011). The whole process is shown in Figure 6, and the test results are shown in Figure 7, with the yellow line indicating design strength of the lining. Only 12.6% of the measured samples from the two sections reached or exceeded the design value in terms of strength. The maximum value was 29.4 MPa; this may be due to the initial stage of sulfate corrosion and carbonation, which made the reaction products fill the pores of the concrete, thereby reducing the porosity, and increasing the density and strength. The lowest strength was only 10.9 MPa, which was lower than the design value.

3.2 Core strength test

In the zones of Z1 and Z2 where the lining was seriously corroded or the surface could not be easily measured using the rebound method, a core drilling machine was used to test the strength of core, as shown in Figure 8; 60 test samples in Z1 and 88 in Z2 were tested. The test results after removing the data with a large degree of discretization are shown in

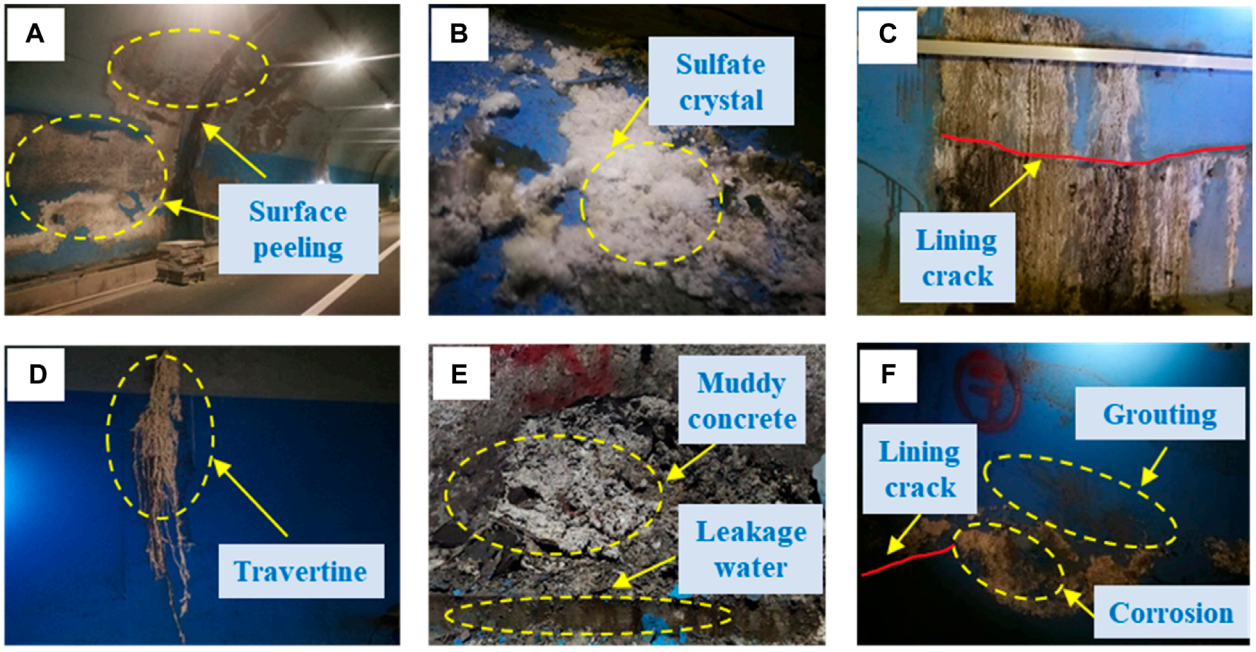

FIGURE 5
Corrosion of the tunnel lining: **(A)** surface peeling; **(B)** sulfate crystal; **(C)** lining crack corrosion; **(D)** travertine; **(E)** muddy concrete; **(F)** grouting repair site corrosion.

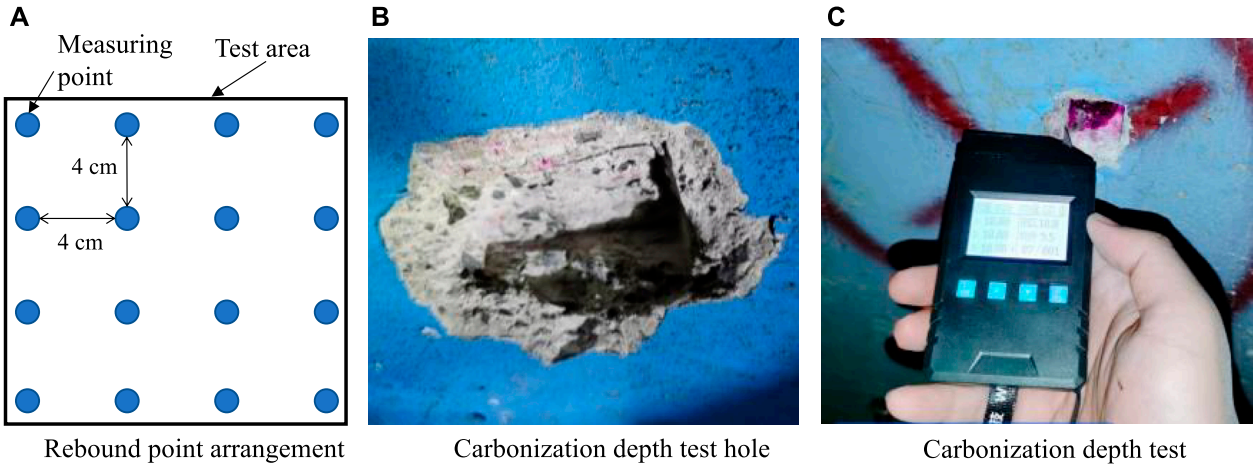

FIGURE 6
Measurement of the tunnel lining strength using the rebound method: **(A)** rebound point arrangement; **(B)** carbonization depth test hole; **(C)** carbonization depth test.

Figure 9, with the yellow line indicating the design strength of the lining.

The average strength of Z1 was 25.12 MPa, 50% of which met or exceed the design standard, and the maximum strength was 31.2 MPa. The reason for this phenomenon may be that part of the core sample came from the lining surface, which had not been corroded, and due to carbonization, the compressive strength increased. However, the lowest strength was only 14.9 MPa, which only reached 59.6% of the designed strength, indicating that the deterioration of the lining was not uniform, and this would lead to stress concentration.

The average strength of Z2 was 22.1 MPa, and only 21.6% reached the design strength, with a maximum value of 30.5 MPa and a minimum value of 13.0 MPa. This indicated that the lining corrosion of Z2 was more serious than that of Z1. After the lining was corroded, the lining material deteriorated seriously, and the lowest strength was only 52% of the designed strength. The safety factor of the structure was greatly reduced, and there were hidden risks that compromised operation safety.

The average value of the core strength of the two corrosion sections was larger than the average value of the strength measured by the rebound method. The reason for this phenomenon was not

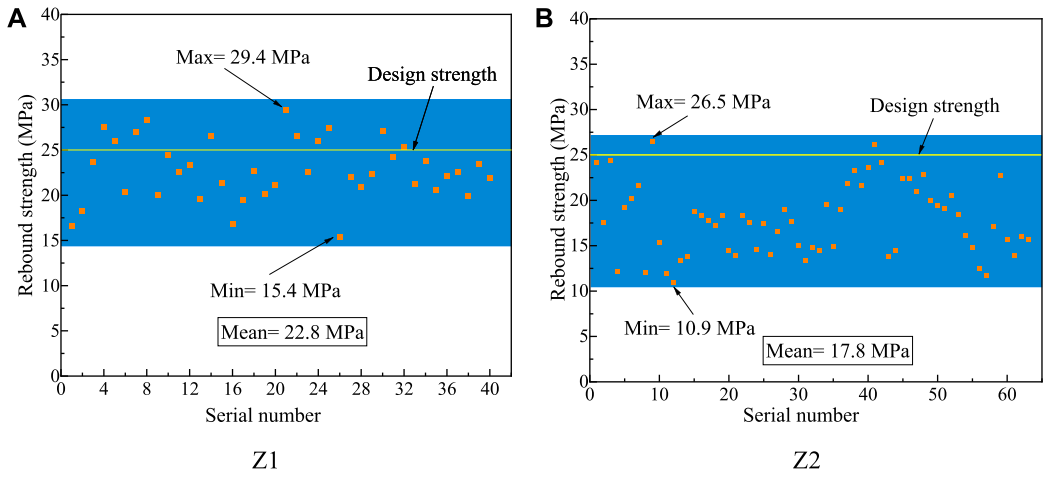

FIGURE 7
Rebound strength of the corroded lining at Z1 **(A)** and Z2 **(B)**.

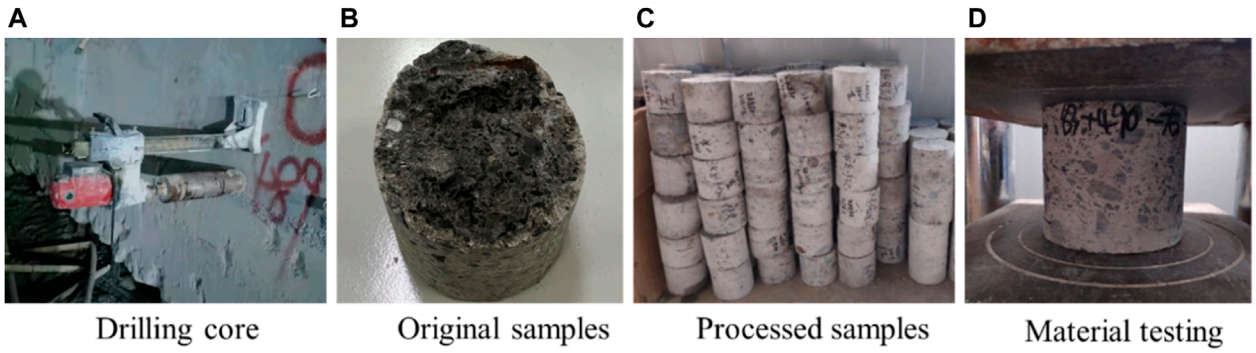

FIGURE 8
Drill core test of the corroded lining: **(A)** drilling core; **(B)** original samples; **(C)** processed samples; **(D)** material testing.

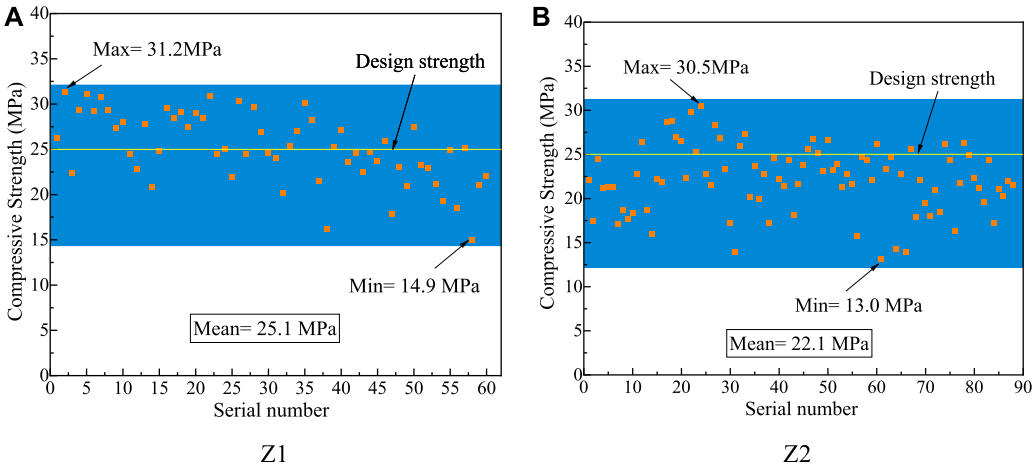

FIGURE 9
Core strength of the corroded lining at Z1 **(A)** and Z2 **(B)**.

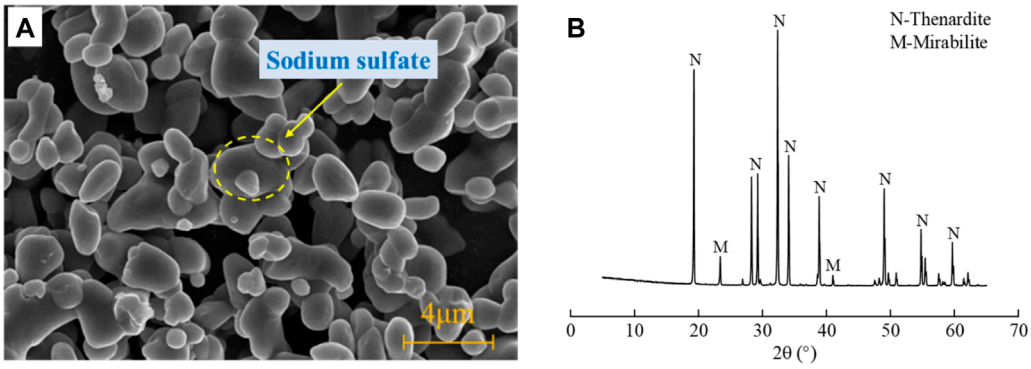

FIGURE 10
Microstructure **(A)** and XRD pattern **(B)** of the soft white crystals.

only related to the measurement error and the fact that part of the core sample analyzed above was from the carbonized surface, but also because some of the core samples were from the corrosion crack, which had been repaired by grouting, and thus the strength of the secondary lining concrete there was improved. However, in general, different degrees of material deterioration occurred in the secondary lining of the two corroded sections, which affected the safety of the structure.

3.3 Analysis of the corrosion products

To further explore the corrosion mechanism of the tunnel lining, samples were taken from the soft white crystallites on the surface (Figure 5B), hard travertine products at the cracks (Figure 5D), corroded lining concrete with strength (Figure 5A), and muddy corroded lining without strength at the arch foot (Figure 5E). Scanning electron microscopy (SEM), energy-dispersive X-ray spectroscopy (EDS), Fourier transform infrared spectrometry (FTIR), and powder X-ray powder diffraction (XRD) were used to investigate the micromorphology and chemical products of the tunnel lining after sulfate corrosion.

3.3.1 White crystals on the surface

Figure 10 shows the results of SEM and XRD analysis of the white crystals. It can be observed that the white crystals were mainly sodium sulfate crystals, and their microscopic morphology is shown in Figure 10A, with a diameter of 0.2–2 μm. According to the XRD pattern (Figure 10B), the white crystals were mainly a mixture of thenardite (Na2SO4) and mirabilite (Na2SO4·10H2O), and the thenardite content was higher.

3.3.2 Travertine

The SEM, EDS, and XRD images of travertine are shown in Figure 11. SEM images showed that the crystal shape was scaly in shape. EDS analysis showed that the main components of travertine were Ca, Si, O, and C, with a small amount of Mg, Al, and Na. The XRD results showed that the main phase of travertine was calcium carbonate, with a small amount of gypsum and quartz, which was consistent with the EDS results.

3.3.3 Corroded lining concrete

The results of SEM, EDS, and XRD of corroded lining concrete of strength are shown in Figure 12. As can be observed in Figures 12A, B, needle-rod and massive crystals were produced in the lining concrete corroded by sulfate. EDS analysis revealed that the elements Ca, Al, S, O, C, and Si were present in the needle-rod crystals, while the elements Ca, S, O, and Na were present in the massive crystals. XRD revealed that the needle-rod crystals were ettringite, whereas the massive crystals were gypsum. After sulfate had corroded the concrete, common corrosion products such as ettringite and gypsum were produced, demonstrating that conventional chemical corrosion occurred in the tunnel lining.

The shape of the muddy corroded lining without strength at the arch foot was completely different from that of ordinary sulfate-corroded concrete. Thus, it can be initially assumed that the corrosion products were not conventional ettringite or gypsum. Figure 13A shows the SEM and EDS images of the muddy corroded lining, and Figure 13B shows the XRD images. The XRD patterns show that thaumasite, ettringite, calcite, gypsum, and a small amount of quartz were present in the samples. As the characteristic peaks of thaumasite (0.956 nm, 0.551 nm, 0.467 nm, 0.387 nm, etc.) were basically consistent with those of ettringite (0.972 nm, 0.561 nm, 0.486 nm, 0.387 nm, etc.) (Barnett et al., 2002), the diffraction peaks of the two have high overlap in the XRD pattern; therefore, it is difficult to distinguish them with XRD (Ma et al., 2012). The SEM image shows that there were many needle-rod crystals with a diameter of 0.5 μm and a length of 3–4 μm in the muddy products, but it was still impossible to identify thaumasite or ettringite. The EDS image showed the presence of O, S, Si, and Ca but not Al, indicating that there was almost no ettringite. Therefore, it can be initially determined that the corrosion product appeared to be thaumasite. However, amorphous phases associated with thaumasite and ettringite crystals can lead to erroneous EDS analysis results (Barnett et al., 2002).

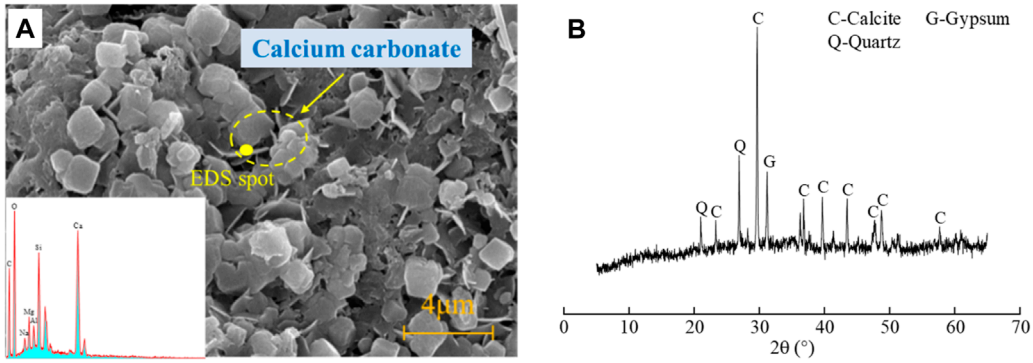

FIGURE 11
Microstructure, EDS analysis **(A)**, and XRD pattern **(B)** of travertine.

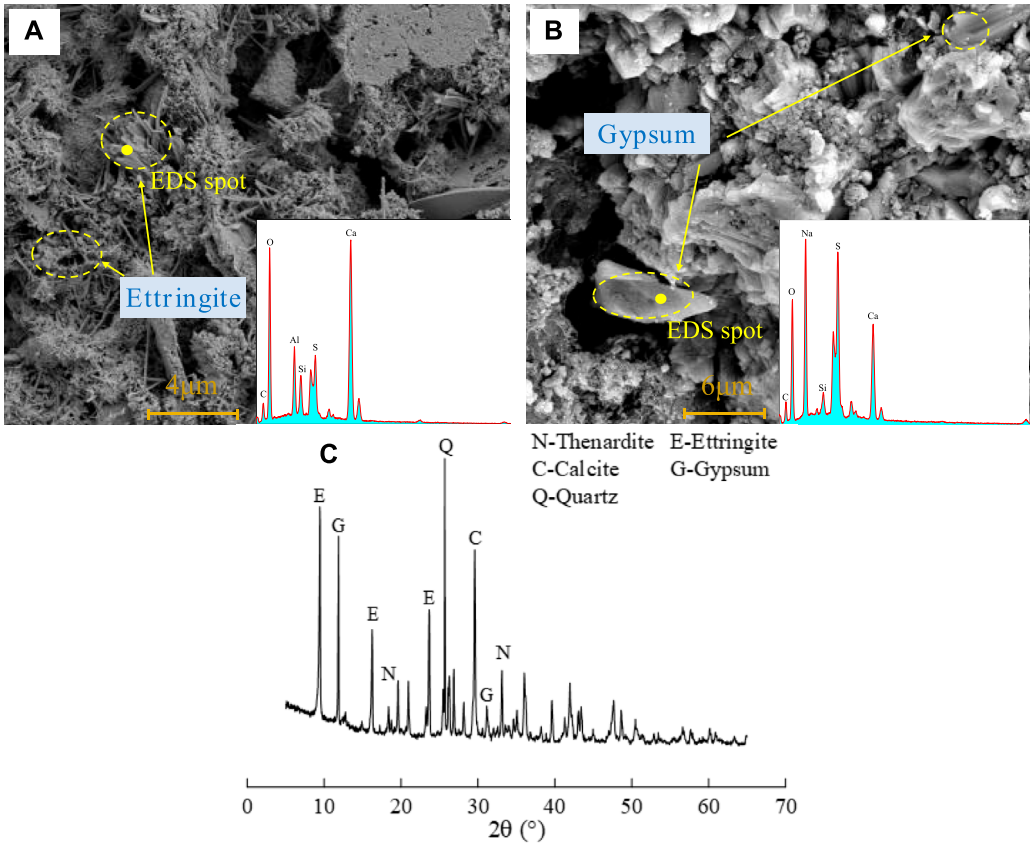

FIGURE 12
Microstructure, EDS analysis **(A,B)**, and XRD pattern **(C)** of the corroded lining concrete of strength.

To further determine the muddy corrosion products, the residual powder samples were analyzed by FTIR. The FTIR spectra are shown in Figure 13C, and the wavenumber of important infrared absorption bands refers to the available data (Ma et al., 2019). The results showed that there was a C-O stretching vibration at approximately 1,400 cm^{-1}, indicating the presence of CO32-. In addition, there was a S-O stretching vibration at approximately 1,100 cm^{-1}, indicating the presence of SO42-. Moreover, a peak was detected at 497 cm^{-1}; this peak was related to the existence of an SiO6 bond. Octahedral silicon is a rare coordination state for mineral silicates. Therefore, the existence of this peak indicated the presence of thaumasite or solid solution containing thaumasite. Second, no peak was found at approximately 850 cm^{-1}, indicating the absence of AlO6. The results of FTIR showed that the composition of the muddy lining concrete was mainly

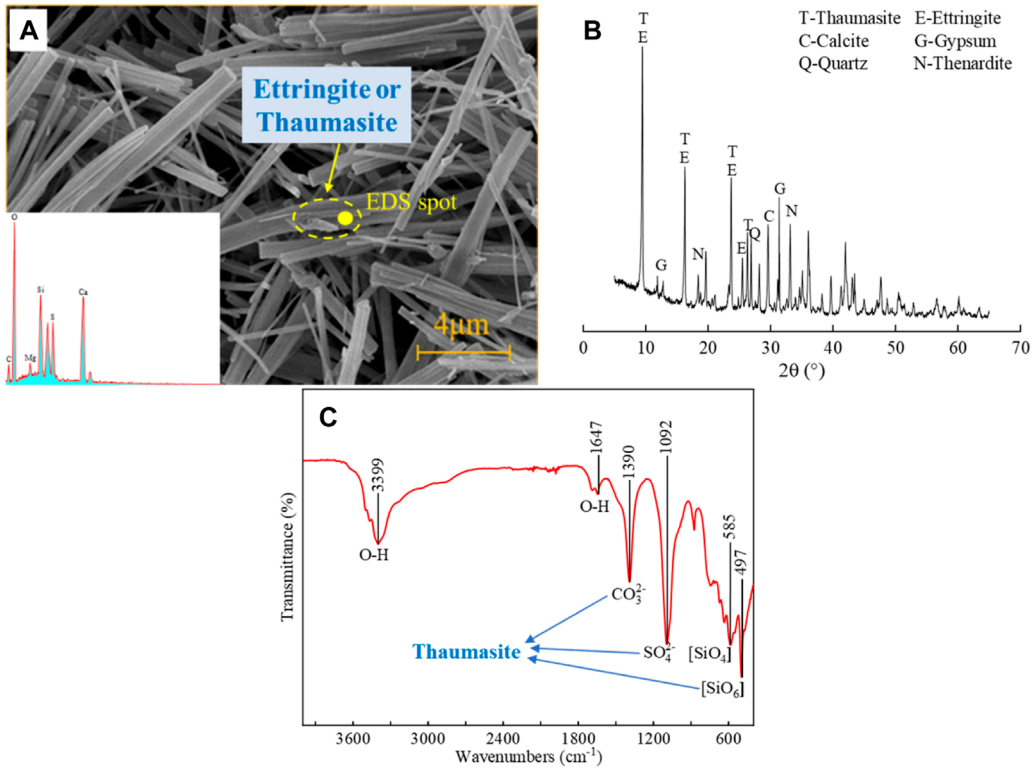

FIGURE 13
Microstructure, EDS analysis **(A)**, XRD pattern **(B)**, and FITR analysis **(C)** of muddy corroded lining without strength.

thaumasite. Therefore, a relatively rare sulfate corrosion occurred in the tunnel.

4 Discussion

4.1 The typical corrosion environment of tunnel lining

In the last century, there were relevant reports on sulfate-corroded tunnels. The main corrosion causes of some sulfate-corroded tunnels are shown in Table 1. Based on the above research results and Table 1, it can be found that the current reports on tunnel damage in a sulfate environment were mainly concentrated in China. Figure 14 shows the regional statistics of the sulfate-corroded tunnels in China featured in Table 1. It can be observed that sulfate-corroded tunnels were mainly distributed in Southwest China and Northwest China. This was because, in Southwest China, the geological conditions are complex, the topography is large, and the salt-bearing strata are widely distributed. Some mountain tunnels are located in areas with a lot of groundwater and gypsum rock. Under the influence of groundwater, corrosive minerals such as gypsum rock will dissolve and produce sulfate, which makes the water environment of tunnel lining contain a large number of sulfate ions, resulting in lining corrosion. At the same time, Southwest China is a tropical monsoon climate area, with a temporal and spatial precipitation distribution that is not uniform, which exposes the lining to dry and wet cycles over a long period, and this will contribute to increasing the sulfate concentration in the environment of the lining, accelerating sulfate corrosion. Moreover, there are many salt lakes and saline soils in Northwest China, and these areas are full of corrosive ions such as sulfate and chloride ions, which will cause compatible corrosion. At the same time, the low winter temperature in this region subjects the lining structure to a freeze-thaw cycle, which damages the concrete lining and accelerates sulfate corrosion.

At the same time, Table 1 shows that the groundwater in the sulfate-corroded tunnel is generally rich, and the sulfate content in the groundwater is high. The main source of sulfate may be sulfur-containing minerals (such as gypsum and mirabilite) and organic matter (such as petroleum and coal) in the surrounding rock, which will be dissolved in the groundwater or even react with the groundwater, or it may be an external pollution resource. In some tunnel linings, the concrete mix contains sulfates, causing the lining to corrode from the inside. In addition, some coupling effects (such as the wet-dry cycle, freeze-thaw cycle, and high geothermal temperature) also accelerate the corrosion of tunnel lining by sulfate.

At present, most scholars have adopted the full-immersion corrosion mode for sulfate erosion of concrete (Liang et al., 2022; Lu et al., 2022; Zhang et al., 2022), and the corrosion mechanism in this corrosion mode has been relatively clear: chemical corrosion

TABLE 1 Sulfate-corroded tunnels and the main cause of their corrosion.

Tunnels	The main cause of corrosion
Luodai Tunnel	The leachate of landfill near the upstream of the tunnel contains sulfate ions (Zhang, 2019)
Fenjieliang Tunnel and Tanjiazhai Tunnel	The corroded section of the tunnel is located in the Badong Formation of the Triassic system, in which gypsum mineral is rich. Groundwater is developed in the section with severe local erosion, and the sulfate content was high in a water quality test (Peng, 2018)
Zagros Tunnel	The tunnel passes through organic-containing strata (oil and coal) with abundant H_2S and water (Salmi et al., 2019)
Fala Tunnel	The groundwater is rich in sulfate, and pulverized coal adheres to the lining surface when trains carrying coal pass through (Long et al., 2011)
Liupanshan Tunnel	The contents of sulfate, chloride ion, and bicarbonate in the tunnel leakage are high (Jiang et al., 2007), and the water quality at the same point is deteriorating constantly. The freeze-thaw cycle accelerates the lining damage (Zhang and Huang, 2012)
Shiziya Tunnel	Gypsum dolomite aggregate causes sulfate erosion in the concrete (Xing et al., 2014). Acid sulfate is produced after karst erosion of anhydrite in the strata where the tunnel is located (Liu et al., 2011)
Jinjiguan Tunnel	Gypsum dissolves in water to produce sulfate in the formation (Qi et al., 2005)
Gaoligong Mountain Tunnel	Highland heat and sulfate coupling (He, 2016)
Pandaoling Tunnel	The groundwater contains higher sulfate, and the freeze-thaw cycle accelerates the corrosion (Yin, 2016)
Ninadu Tunnel	The area where the tunnel is located has a large number of coal seams and abundant surface water and groundwater containing high levels of sulfate (Liu and Sun, 2009)
Jiaozi Mountain Tunnel	Rock salts such as gypsum, Glauber, and chloride are developed in the rock strata surrounding the tunnel. In the water environment, sulfate and chloride ions are ionized by rock salts (Liu, 2018)
Baijialing Tunnel	The stratum where the tunnel is located is rich in gypsum, and the dry-wet cycle accelerates the corrosion (Han, 1999)
Koblenz Tunnel	Sulfate in surrounding rock and groundwater (Romer, 2003)
Jiaozhou Bay Subsea Tunnel	The seawater in the area where the tunnel is located has high levels of sulfate, chloride, and magnesium ions, and the lining is in an alternating wet and dry environment, which accelerates the corrosion (Liu, 2008)
Podixia Tunnel	Sulfate ion concentration in the groundwater exceeds the corrosion resistance index of sulfate-resistant cement (Cai, 1986)
Qinling Tunnel	Abnormal groundwater, in which the levels of sulfate ions, salinity, and calcium ions increased significantly (Wang et al., 2002)
Dajiangkou Tunnel and XinXuefeng Mountain Tunnel	Sulfate content in the leakage water is at a level that is moderately corrosive, and the construction quality is problematic (Sun et al., 2004)

mainly occurs, and its corrosion products are gypsum and ettringite, which is the conventional sulfate corrosion. However, some scholars have found that the corrosion mechanism of concrete will change when concrete is in semi-immersion mode (Zhang et al., 2020a; Zhang et al., 2022).

Therefore, combined with the field investigation results, it can be concluded that compared with conventional sulfate corrosion, tunnel lining is in a special state of "one-sided accelerated corrosion" as shown in Figure 15: the inner side of the tunnel lining is in contact with groundwater containing sulfate, resulting in unilateral corrosion under a wet-dry cycle. Furthermore, the outside part of the lining is in contact with the air, which leads to water evaporation on the lining surface; this will accelerate the transfer of sulfate from the inside to the outside and consequently subject the tunnel lining to both physical and chemical sulfate corrosion, and the whole process will be accompanied by carbonization.

4.2 The mechanisms of one-sided accelerated corrosion on tunnel lining

4.2.1 Physical corrosion

With the appearance of sodium sulfate crystals on the surface of the lining, it can be inferred that the tunnel lining had been subjected to physical corrosion. The reason for this phenomenon was because the tunnel lining was in a "one-sided accelerated corrosion" state: the inside part was in contact with corrosive groundwater, while the outside part was in contact with air. In this case, the inner side of the area in contact with the groundwater permitted the sulfate to enter the lining, while the outer side, which was in contact with the air, constituted an evaporation area. The sulfate solution migrated from the inside to the outside due to capillary suction and diffusion, while the outside part was supersaturated due to water evaporation, and the sulfate solution precipitated out. When the sulfate precipitated out, the resulting

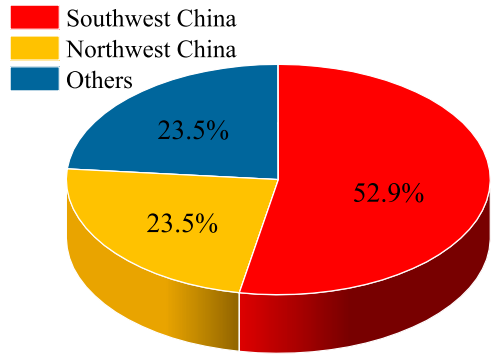

FIGURE 14
Distribution of some sulfate-corroded tunnels in China.

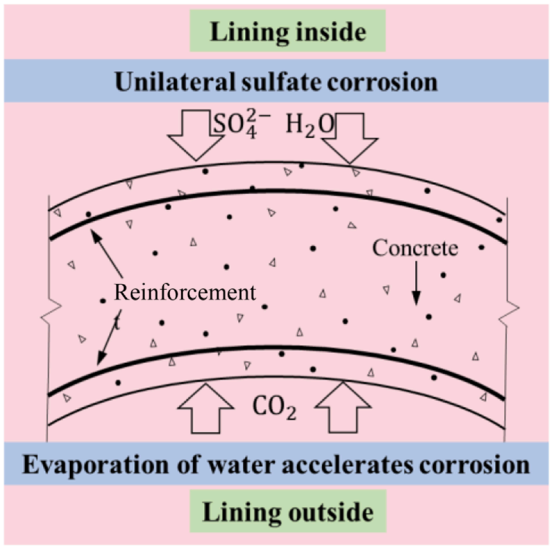

FIGURE 15
One-sided accelerated corrosion of tunnel lining.

concentration difference pushed the inner sulfate solution to migrate outward. When the pressure of sulfate crystallization exceeds the tensile strength of the concrete, it will damage the concrete. This type of corrosion is called physical corrosion. On the other hand, the tunnel is located in an area of seasonal precipitation, which means that in the rainy season, the groundwater containing sulfate would come into contact with the lining inside. In the dry season, the lining was relatively dry. Thus, the tunnel lining was also in a wet-dry cycle, and this would accelerate the physical corrosion.

4.2.2 Chemical corrosion

4.2.2.1 Soluble chemical corrosion

The generation of travertine indicated that the tunnel lining had undergone soluble chemical corrosion, and this was due to the following reasons: first, under the influence of underground water, the $Ca(OH)_2$ in the cement constantly dissolved from inside to outside, and the outside of the tunnel was in contact with the air, where CO_2 reacted with $Ca(OH)_2$ to form $CaCO_3$, which was almost insoluble in water (Liu et al., 2015). Then CO2 reacted with $CaCO_3$ in the surface layer and dissolved it to form Ca2+ and HCO_3^-. When Ca^{2+} and HCO_3^- were carried by leakage water from cracks to the lining surface, travertine was formed again due to a sudden drop in pressure (Li and Zhou, 1996). When the crystallization pressure was greater than the tensile strength of the concrete, the lining surface would crack or flake off.

4.2.2.2 Ettringite- and gypsum-type chemical corrosion

The presence of ettringite and gypsum, which were found in the lining concrete, proved that the tunnel lining had been subjected to ettringite- and gypsum-type chemical corrosion, which are the most common corrosion mechanisms in sulfate-corroded concrete.

4.2.2.3 Thaumasite-type chemical corrosion

The muddy concrete was thaumasite, which proved that rare thaumasite-type chemical corrosion occurred in the tunnel. Currently, it is generally believed that the five conditions of carbonite, silicate, carbonate, sufficient water, and low temperature need to be met for thaumasite sulfate corrosion to occur (Crammond, 2003). The content of sulfate ions in the groundwater was sufficient. The design data showed that Portland cement was used as the secondary lining concrete of the tunnel, and C-S-H gel, which was produced after hydration, was the main source of silicate. The aggregate in concrete was mostly limestone, and the carbonized concrete was the main source of carbonate. Water leakage provided ample water for corrosion. Although existing studies had shown that thaumasite is easily generated when the temperature is lower than 15°C, especially at 0°C–5°C, and the average annual temperature of the tunnel site was approximately 16.4°C, some scholars found that thaumasite can also be generated when the temperature is higher than 15°C (Diamond, 2003). When all of this is considered, it can be concluded that the tunnel environment created the conditions for the formation of thaumasite.

4.2.3 Damage mechanism

Different from the full-immersion test in the laboratory, physical and chemical corrosion occurred in the tunnel lining in the actual environment because of one-sided accelerated corrosion. The chemical corrosion consumed the cementing matrix of cement slurry, damaged the cementing structure of the concrete, reduced the bond between the aggregate, and then greatly reduced the concrete compactness and bearing capacity. The corrosion products generated by chemical and physical corrosion accumulated continuously in the pores of concrete and squeezed the pores, resulting in pore tip or pore wall cracking. As the corrosion continued, a large number of cracks were generated, and then new defects such as through-cracks were formed, which increased the lining damage, as shown in Figure 16.

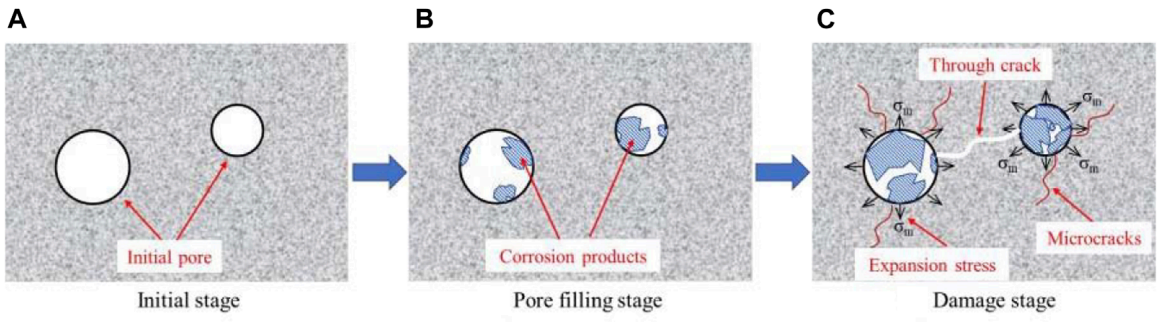

FIGURE 16
Diagram of the whole process of sulfate corrosion in concrete: **(A)** initial stage; **(B)** pore filling stage; **(C)** damage stage.

5 Conclusion

Based on a sulfate-corroded highway tunnel in Southwest China, this study analyzed the damage characteristics of tunnel lining in a sulfate environment through field investigation and laboratory tests. Moreover, this study summarized the typical working environment and corrosion mechanism of a tunnel under sulfate attack by combining the results with an analysis of existing reports related to sulfate-corroded tunnels. The main conclusions are as follows.

(1) The leakage position of the tunnel was concentrated mainly in the arch foot and arch waist and mostly in the lining cracks or corrosion area. It was found that sulfate ions were the main corrosive ions in the tunnel leakage water, which was at a moderate-to-serious corrosion level.
(2) The lining of the tunnel had been subjected to serious corrosion, which manifested as a large area of surface shedding, surface crystallization, and travertine. The concrete in some areas of the arch foot was muddy, and the corrosion degree was higher at cracks. The areas repaired with grouting had become corroded again.
(3) The strength of most of the tested areas was lower than the designed value. The strength of a small part of the tested area was higher than the design value, which may be due to the decrease in the porosity of the concrete lining and increase in strength at the early stage of carbonization or sulfate corrosion.
(4) The white crystals on the surface were mainly thenardite. The travertine was mainly calcium carbonate. Ettringite and gypsum were detected in the corroded lining concrete, and the muddy concrete in the arch foot was thaumasite.
(5) The sulfate-corroded tunnels in China are mainly distributed in the Southwest and Northwest. The common feature of the tunnels is that the soil and rock strata are rich in groundwater and contain a large number of sulfur-containing substances, such as gypsum salt and coal, which dissolve in groundwater or react with it to form sulfate ions, and this is the direct cause of lining structure corrosion.
(6) The special environment of the tunnel lining rendered it in a state of "one-sided accelerated corrosion," which causes physical and chemical corrosion and accelerates the damage to the lining concrete.

Data availability statement

The original contributions presented in the study are included in the article/Supplementary Material, further inquiries can be directed to the corresponding authors.

Author contributions

XL: Conceptualization, Investigation, Methodology, Project administration, Validation, Writing–review and editing. YZ: Data curation, Formal Analysis, Investigation, Methodology, Writing–original draft, Writing–review and editing. XZ: Data curation, Methodology, Project administration, Supervision, Writing–review and editing. NL: Data curation, Investigation, Project administration, Supervision, Validation, Writing–original draft. JM: Data curation, Investigation, Writing–original draft. HC: Investigation, Writing–original draft.

Funding

The author(s) declare financial support was received for the research, authorship, and/or publication of this article. This study is supported by the National Natural Science Foundation for Young Scientists of China (Grant No. 52104076), the Science and Technology Foundation of the Department of Transportation of Zhejiang Province, China (Grant No. 2020028).

Acknowledgments

Additionally, editors and reviewers proposed helpful and pertinent comments. The authors gratefully acknowledge this support.

Conflict of interest

The authors declare that the research was conducted in the absence of any commercial or financial relationships that could be construed as a potential conflict of interest.

Publisher's note

References

Barnett, S. J., Macphee, D. E., Lachowski, E. E., and Crammond, N. J. (2002). XRD, EDX and IR analysis of solid solutions between thaumasite and ettringite. *Cem. Concr. Res.* 32 (5), 719–730. doi:10.1016/s0008-8846(01)00750-5

Cai, X. Z. (1986). Discussion on anti-corrosion of railway tunnel invert. *Railw. Eng.* (01), 12–16.

Chen, J. K., Jiang, M. Q., and Zhu, J. (2008). Damage evolution in cement mortar due to erosion of sulphate. *Corros. Sci.* 50 (9), 2478–2483. doi:10.1016/j.corsci.2008.05.021

Crammond, N. (2002). The occurrence of thaumasite in modern construction - a review. *Cem. Concr. Comp.* 24 (3-4), 393–402. doi:10.1016/s0958-9465(01)00092-0

Crammond, N. J. (2003). The thaumasite form of sulfate attack in the UK. *Cem. Concr. Comp.* 25 (8), 809–818. doi:10.1016/s0958-9465(03)00106-9

Diamond, S. (2003). Thaumasite in Orange County, Southern California: an inquiry into the effect of low temperature. *Cem. Concr. Comp.* 25 (8), 1161–1164. doi:10.1016/s0958-9465(03)00138-0

Han, T. C. (1999). Evaluation for concrete corrosion of baijialing tunnel. *Chin. Railw.* 1999 (8), 29–31+25.

He, M. M. (2016). *The influence of heat sulfate solution to mechanics performance of concrete*. Chengdu, China: Southwest Jiaotong University.

Hobbs, D. W., and Taylor, M. G. (2000). Nature of the thaumasite sulfate attack mechanism in field concrete. *Cem. Concr. Res.* 30 (4), 529–533. doi:10.1016/s0008-8846(99)00255-0

Jiang, W. D., Chen, X., and Liu, B. (2007). Analysis and treatment of lining concrete corrosion failure in Liupanshan Tunnel. *J. Highw. Transp. Res. Dev.* 24 (10), 108–112.

Lee, S. T., Hooton, R. D., Jung, H. S., Park, D. H., and Choi, C. S. (2008). Effect of limestone filler on the deterioration of mortars and pastes exposed to sulfate solutions at ambient temperature. *Cem. Concr. Res.* 38 (1), 68–76. doi:10.1016/j.cemconres.2007.08.003

Li, D. L., and Zhou, Z. A. (1996). Possibility of corrosion failure of comcrete shaftwall due to water infiltration. *J. China Coal Soc.* 21 (2), 158–163.

Liang, N. H., Mao, J. W., Yan, R., Liu, X., and Zhou, X. (2022). Corrosion resistance of multiscale polypropylene fiber-reinforced concrete under sulfate attack. *Case Stud. Constr. Mater.* 16, e01065. doi:10.1016/j.cscm.2022.e01065

Liu, J. H., Bian, L. B., He, W., and Ji, H. G. (2015). Investigation and destruction mechanism on corrosion of concrete shaft in coal mine. *J. China Coal Soc.* 40 (03), 528–533.

Liu, W. (2008). *Research on durability of lining concrete of qingdao jiaozhou bay submarine tunnel*. Qingdao, China: Qingdao Technological University.

Liu, X. R., Zhuang, Y., Zhou, X. H., Li, C., Lin, B. B., Liang, N. H., et al. (2023). Numerical study of the mechanical process of long-distance replacement of the definitive lining in severely damaged highway tunnels. *Undergr. Space* 9, 200–217. doi:10.1016/j.undsp.2022.07.007

Liu, Y. M. (2018). Anti-corrosion construction technique research for tunnel with complex formation at halite area. *Constr. Technol.* 47 (16), 56–60+139.

Liu, Y. M., Yu, H. M., Wang, C., and Wang, C. L. (2011). Research on mechanism of damage of anhydrock in dolomite layer to tunnel structure. *Rock Soil Mech.* 32 (9), 2704–2708+2752.

Liu, Z. Q., and Sun, S. Q. (2009). "Analysis of sulfate corrosion of concrete in Ninadu Tunnel and its prevention measures," in Proceedings of the 3rd Conference of Geo-Engineering, Chengdu, Sichuan, China, October, 2009.

Long, G. C., Xie, Y. J., Deng, D. H., and Li, X. K. (2011). Deterioration of concrete in railway tunnel suffering from sulfate attack. *J. Central South Univ. Technol.* 18 (3), 881–888. doi:10.1007/s11771-011-0777-4

Lu, F., Wang, H., Wang, L., Zhao, K., and Zhang, J. (2022). Degradation law and service life prediction model of tunnel lining concrete suffered combined effects of sulfate attack and drying-wetting cycles. *Materials* 15 (13), 4435. doi:10.3390/ma15134435

Ma, B. G., Gao, X. J., Byars, E. A., and Zhou, Q. Z. (2019). Thaumasite formation in a tunnel of bapanxia dam in Western China. *Cem. Concr. Res.* 36 (4), 716–722. doi:10.1016/j.cemconres.2005.10.011

Ma, K. L., Long, G. C., and Xie, Y. J. (2012). Railway tunnel concrete lining damaged by formation of gypsum, thaumasite and sulfate crystallization products in southwest of China. *J. Cent. South Univ.* 19 (8), 2340–2347. doi:10.1007/s11771-012-1280-2

Peng, Z. L. (2018). *Study on the coupling effect of hydrological-chemical-mechanical in deep buried tunnel with gypsum salt and its prevention and control countermeasures*. Chongqing, China: Chongqing Jiaotong University.

Qi, J. H., Hou, Z. L., Jia, S. Y., and Wang, N. F. (2005). The research on the characteristics of Jinjiguan Tunnel's water penetration and deformation with defects control measures. *J. Disaster Prev. Mitig. Eng.* 25 (2), 222–226.

Romer, M. (2003). Steam locomotive soot and the formation of thaumasite in shotcrete. *Cem. Concr. Comp.* 25 (8), 1173–1176. doi:10.1016/s0958-9465(03)00155-0

Salmi, E. F., AsadiBayati, Z. S. M., and Sharifzadeh, M. (2019). Assessing the hydrogeological conditions leading to the corrosion and deterioration of pre-cast segmental concrete linings (case of zagros tunnel). *Geotechnical Geol. Eng.* 37 (5), 3961–3983. doi:10.1007/s10706-019-00886-1

Sun, Y. B., Yu, G. X., and Wang, H. (2004). The sulfate attack on the lining concrete in tunnel and it's renovation engineering. *J. Railw. Eng. Soc.* (04), 89–92+88.

Wang, J. X., Liu, D., and Yang, L. Z. (2002). Evaluation and prevention of concrete erosion caused by chemical abnormity of groundwater in Qinling tunnel. *Mod. Tunn. Technol.* 39 (4), 33–36.

Xing, Z. S., Deng, M., Wang, A. G., and Liu, K. C. (2014). Internal sulfate attack on concrete caused by gypsum-bearing aggregates. *J. Build. Mater.* 17 (1), 30–34+41.

Yin, T. J. (2014). *Study on causes and treatment technologies of diseases in Pandaoling Tunnel in Datonghe-Qingwangchuan diversion project*. Lanzhou, China: Lanzhou Jiaotong University.

Zhang, J., and Huang, H. (2012). Comprehensive improvement of the liupanshan tunnel disease. *Energy Energy Conservation* (10), 89–91.

Zhang, Z. Y. (2019). *Mesoscopic erosion mechanism and shear properties of shotcrete materials under sulfate-containing environments*. Chongqing, China: Chongqing University.

Zhang, Z. Y., Jin, X. G., and Luo, W. (2019). Numerical study on the collapse behaviors of shallow tunnel faces under open-face excavation condition using mesh-free method. *J. Eng. Mech.* 145 (11), 04019085. doi:10.1061/(asce)em.1943-7889.0001661

Zhang, Z. Y., Pang, K., Xu, L. H., Zou, Y., Yang, J., and Wang, C. B. (2023). The bond properties between UHPC and stone under different interface treatment methods. *Constr. Build. Mater* 365, 130092. doi:10.1016/j.conbuildmat.2022.130092

Zhang, Z. Y., Zhou, J. T., Yang, J., Zou, Y., and Wang, Z. S. (2020b). Cracking characteristics and pore development in concrete due to physical attack. *Mater Struct.* 53 (4), 104. doi:10.1617/s11527-020-01541-5

Zhang, Z. Y., Zhou, J. T., Zou, Y., Yang, J., and Bi, J. (2020a). Change on shear strength of concrete fully immersed in sulfate solutions. *Constr. Build. Mater* 235, 117463. doi:10.1016/j.conbuildmat.2019.117463

Zhang, Z. Y., Zou, Y., Yang, J., and Zhou, J. T. (2022). Capillary rise height of sulfate in Portland-limestone cement concrete under physical attack: experimental and modelling investigation. *Cem. Concr. Comp.* 125, 104299. doi:10.1016/j.cemconcomp.2021.104299

Zhuang, Y., Liu, X. R., Zhou, X. H., and Du, L. B. (2022). Diffusion model of sulfate ions in concrete based on pore change of cement mortar and its application in mesoscopic numerical simulation. *Struct. Concr.* 23 (6), 3786–3803. doi:10.1002/suco.202100760